Catalysis Today 164 (2011) 302–307

Contents lists available at ScienceDirect

Catalysis Today

journal homepage: www.elsevier.com/locate/cattod

Effect of nanocrystalline χ-Al_2O_3 structure on the catalytic behavior of Co/Al_2O_3 in CO hydrogenation

Wasu Chaitree[a], Sirithan Jiemsirilers[b], Okorn Mekasuwandumrong[c], Bunjerd Jongsomjit[a], Artiwan Shotipruk[a], Joongjai Panpranot[a,*]

[a] Department of Chemical Engineering, Faculty of Engineering, Chulalongkorn University, Bangkok 10330, Thailand
[b] Department of Materials Science, Faculty of Science, Chulalongkorn University, Bangkok 10330, Thailand
[c] Department of Chemical Engineering, Faculty of Engineering and Industrial Technology, Silpakorn University, Nakorn Phathom 73000, Thailand

ARTICLE INFO

Article history:
Available online 8 December 2010

Keywords:
χ-Al_2O_3
Cobalt catalyst
CO hydrogenation
Solvothermal
Gibbsite

ABSTRACT

In the present study, nanocrystalline χ-Al_2O_3 were prepared by thermal decomposition of fine gibbsite (χ-GB) and solvothermal method (χ-SV) and employed as supports for preparation of 20 wt% Co/Al_2O_3 catalysts. As compared to the use of γ-Al_2O_3 with similar BET surface area, Co dispersion and CO hydrogenation activity were higher on the nanocrystalline χ-Al_2O_3 supported Co catalysts. The transmission electron microscopy (TEM) results revealed that the wrinkled sheets-like structure of γ-Al_2O_3 was completely destroyed after CO hydrogenation for 6 h whereas the spherical particles of χ-SV and plate-like structure of χ-GB were maintained. The H_2-temperature program reduction (H_2-TPR) also revealed a stronger interaction between cobalt and alumina supports for the Co/χ-Al_2O_3 catalysts.

1. Introduction

Alumina is the most common inorganic oxide used as catalyst carrier because of its excellent thermal stability and wide range of chemical, physical, and catalytic properties. Various transition alumina (e.g. α-, γ-, χ-, δ-, η- and θ-Al_2O_3) has been prepared by different methods such as, sol-gel synthesis [1,2], hydrothermal synthesis, microwave synthesis [3], emulsion evaporation [4], plasma technique [5], and solvothermal synthesis [6–9]. Among these methods, solvothermal synthesis attracts considerable attention because it gives the products with uniform morphology, well-controlled chemical composition, and narrow size distribution. Furthermore, desire shape and size of particles can be produced by controlling process conditions such as solute concentration, reaction temperature, reaction time, and the type of solvent [10,11]. A number of studies show that highly stable nanocrystalline χ-Al_2O_3 prepared by the solvothermal method exhibited interesting results when employed as catalyst and catalyst supports in many catalytic reactions including CO hydrogenation [12,13], dehydration of methanol to dimethyl ether [14], and CO oxidation [15].

In our recent study, high purity of nanocrystalline χ-Al_2O_3 (100 wt%) was obtained by calcination of milled fine gibbsite at 600 °C and their physical properties were comparable to those produced by the solvothermal method [16]. This offers a simple way to prepare large amount of pure χ-phase alumina for particular industrial applications. In the present work, the effect of χ-Al_2O_3 structure obtained from different routes (i.e. from thermal decomposition of gibbsite and solvothermal method) on the catalytic behavior of Co/Al_2O_3 in the CO hydrogenation reaction was investigated. The commercially obtained γ-Al_2O_3 with similar BET surface area was also employed to prepare the Co/γ-Al_2O_3 as a reference catalyst. The catalysts were characterized by N_2 physisorption, X-ray diffraction (XRD), CO chemisorption, transmission electron microscopy (TEM), and temperature program reduction of H_2 (H_2-TPR). The catalytic behavior of the catalysts was investigated in the CO hydrogenation at 220 °C and atmospheric pressure.

2. Experimental

2.1. Preparation of χ-alumina by thermal decomposition of gibbsite

Approximately 100 g of fine gibbsite (Merck, Germany) was mixed with 300 cm^3 water in a plastic pot and milled in an attrition mill for 24 h, using alumina balls as grinding media. Cooling water was fed continuously in the attrition mill in order to remove heat. Rotational speed of the mill was fixed at 500 rpm. The sample was dried at 105 °C overnight in an oven to remove water. The dried sample was subsequently milled in a mortar to deagglomerate. The sample was calcined in a tube furnace in air (95 ml/min) by heating up to 600 °C at a rate of 10 °C/min and hold at that temperature for

* Corresponding author. Tel.: +66 2218 6869; fax: +66 2218 6877.
E-mail address: joongjai.p@chula.ac.th (J. Panpranot).

0920-5861/$ – see front matter © 2010 Elsevier B.V. All rights reserved.
doi:10.1016/j.cattod.2010.11.004

4 h. Then, the sample was cooled down to room temperature in N_2 (75 ml/min). The sample was denoted as χ-GB.

2.2. Preparation of χ-alumina by the solvothermal method

Nanocrystalline χ-Al_2O_3 was prepared by the solvothermal method according to the procedure described in Ref. [17]. Approximately 15 g of aluminium isopropoxide (AIP) (Aldrich) was suspended in 100 cm^3 of toluene in a beaker, which was then placed in a 300 cm^3 autoclave. In the gap between the beaker and autoclave wall, 30 cm^3 of toluene was added. After the autoclave was completely purged with nitrogen, the suspension was heated to 300 °C at the rate of 2.5 °C/min and held at that temperature for 2 h. Autogenous pressure during the reaction gradually increased as temperature was raised. Then the autoclave was cooled to room temperature. The resulting powder was washed repeatedly with methanol by centrifugation and dried at 110 °C for 24 h. The product was calcined in a box furnace by heating up to 600 °C at a rate of 10 °C/min and held at that temperature for 6 h. The sample was denoted as χ-SV.

2.3. Preparation of Co/Al_2O_3 catalysts

The catalysts were prepared by incipient wetness impregnation with aqueous solution of cobalt(II) nitrate hexahydrate (Aldrich). The certain amount of cobalt (20 wt% loading) was dissolved deionized water and then impregnated onto the support. The catalysts were dried overnight in an oven at 110 °C and then calcined in air at 300 °C for 2 h using a ramp rate of 1 °C/min. The reference Co/γ-Al_2O_3 catalyst was also prepared by the same procedure using the commercially obtained γ-Al_2O_3 (Sumitomo Aluminium Smelting Co. Ltd.) as the catalyst support.

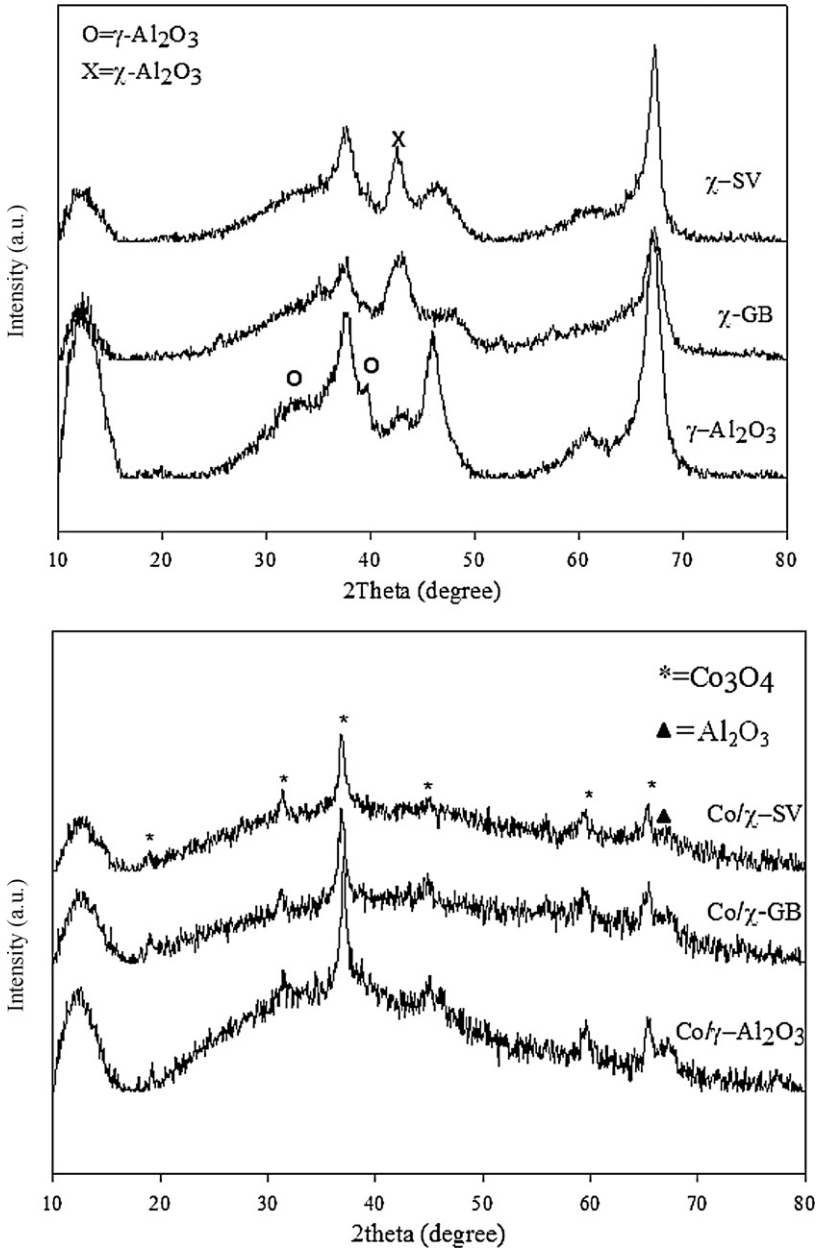

Fig. 1. The XRD patterns of Al_2O_3 and Co/Al_2O_3 catalysts.

Table 1
Physicochemical properties of the Co/Al_2O_3 catalysts prepared on γ- and χ-Al_2O_3.[a]

Samples	Co_3O_4 crystallite size[b] (nm)	Surface area (m^2/g)	Pore volume (cm^3/g)	Average pore diameter (nm)	CO chemisorption (molecule $CO \times 10^{-19}$/g cat)	Co dispersion
Co/χ-SV	8.0	117 (171)	0.38 (0.63)	9.2 (10.4)	2.0	0.29
Co/χ-GB	7.8	135 (183)	0.23 (0.34)	4.9 (4.8)	2.8	0.49
Co/γ-Al_2O_3	9.1	148 (188)	0.35 (0.49)	5.7 (6.8)	1.7	0.19

[a] The number in parenthesis indicate the surface area, pore volume, and average pore diameter of the bare Al_2O_3 supports.
[b] Based on XRD results.

2.4. Catalyst characterization

The X-ray diffraction patterns of the catalysts were measured in a range of 2θ value between 20° and 80° using a SIEMENS D5000 X-ray diffractometer and Cu Kα radiation with a Ni filter. The surface area, pore volume, and average pore diameter were measured by Micromeritics ASAP 2020. The morphology of samples was investigated by TEM (JEOL JEM 2010), operating at 200 kV. The active sites and the relative percentages dispersion of cobalt catalyst were determined by CO pulse chemisorption technique, using Micromeritics ChemiSorb 2750. Prior to the measurements, the catalyst samples were reduced at 350 °C in flowing H_2 for 3 h. TPR was also carried out in a Micrometritics Chemisorb 2750 automated system. The catalyst sample 0.1 g was heated up to 200 °C in flowing nitrogen and held at this temperature for 1 h. The catalyst sample was cooled down to room temperature and the carrier gas was 5% H_2 in Ar (30 cc/min) were ramping from 35 to 800 °C at 10 °C/min. Thermal gravimetric and differential temperature analysis (TG/DTA) were performed using an SDT Analyzer Model Q600 from TA Instruments, USA at heating rate of 5 °C/min in flowing air (400 cm^3/min). The spent catalysts were dried overnight at 110 °C prior to the measurement.

2.5. Reaction study

CO hydrogenation was carried out at 220 °C and 1 atm total pressure in a fixed-bed quartz reactor under differential reaction conditions. The H_2/CO ratio used was 10/1. Typically, 0.1 g of the catalyst sample was reduced *in situ* in flowing H_2 (50 cc/min) at 350 °C for 3 h prior to reaction. After the start up, samples were taken at 1 h intervals and analyzed by gas chromatography. Steady state was reached within 6 h in all cases.

3. Results and discussion

The XRD patterns of the Al_2O_3 supports and the Co/Al_2O_3 catalysts are shown in Fig. 1. The XRD characteristic peaks of γ- and χ-alumina were observed at degree $2\theta = 33°$ and 42.5°, respectively according to the JCPDSs database. According to our previous study, the fraction of χ-phase in both χ-SV and χ-GB was determined to be 100 wt% [12,16]. After Co loading, the diffraction peaks at 2θ of ca. 31.3°, 36.8°, 45.1°, 59.4°, and 65.4° were apparent, indicating that cobalt was primarily in the form of Co_3O_4 spinel after calcination at 300 °C for all the catalyst samples [18]. The physicochemical properties of the Co/Al_2O_3 catalysts prepared on γ- and χ-Al_2O_3 are summarized in Table 1. The BET surface areas of the various Al_2O_3 supports were not significantly different ranging between 171 and 188 m^2/g. As also illustrated in the pore size distribution plots (Fig. 2), the χ-GB possessed the least amount of pore volume and smallest average pore diameter while the χ-SV had the highest pore volume and the largest pore diameter. The γ-Al_2O_3, on the other hand, showed wide pore size distribution in the mesopore range. It is noted that impregnation, drying, and calcination did not change much the pore size distribution as well as the average pore diameter of the cobalt catalysts, but reduced the nitrogen uptake [19]. The calculated crystallite sizes of Co_3O_4 from X-ray line broadening were quite similar for all the catalyst samples (7–9 nm). Such result was in contrast to the work reported previously by Borg et al. [20], in which the largest Co_3O_4 crystallites were found in the support of widest pores. Evidently, the classic model of cylindrical pores with the catalytic component attached to the walls is not valid here. It is shown that the χ-SV with relatively large pore size can result in the formation of small Co_3O_4 crystallites due probably to the fact that χ-SV is single crystal and possesses only interparticle-particle pores. The amount of CO chemisorption as well as the calculated %Co dispersion increased in the order Co/χ-GB > Co/χ-SV > Co/γ-Al_2O_3. The higher Co dispersion on the χ-phase alumina as compared to the higher surface area γ-Al_2O_3 was attributed to the morphology/structure of the Al_2O_3 support. The spherical shape like χ-alumina particles has shown to prevent agglomeration of Co particles on alumina surface, especially at high Co loadings [12,13]. In addition, the bimodal pore structure and the narrow pore size distribution of χ-GB also provided high Co dispersion.

The morphology of the Al_2O_3 supports and the Co/Al_2O_3 catalysts before and after reaction are shown in Fig. 3. The morphology of χ-alumina obtained by thermal decomposition of gibbsite and solvothermal method were apparently different. The χ-SV appeared as very small spherical particles (Fig. 3a) whereas the χ-GB consisted of irregular and flaky particles (Fig. 3d) which were probably the results of milling of the pseudohexagonal plate-like gibbsite [21]. The γ-Al_2O_3 (Fig. 3g) exhibited the wrinkled sheets-like structure similar to that of boehmite [22]. It was found that the spherical and plate-like structure of χ-SV and χ-GB as well as the cobalt dispersion on these χ-phase alumina were maintained after the CO hydrogenation reaction for 6 h whereas the wrinkled sheets-like structure of γ-Al_2O_3 was completely destroyed (Fig. 3c, f, i, respectively). It is noted that the wrinkled sheets structure of γ-Al_2O_3 was still observed after impregnation and calcination of Co/γ-Al_2O_3 (Fig. 3h). The results in this study clearly show that the textural properties of χ-phase alumina were more stable than the γ-Al_2O_3 during CO hydrogenation. It has been reported that

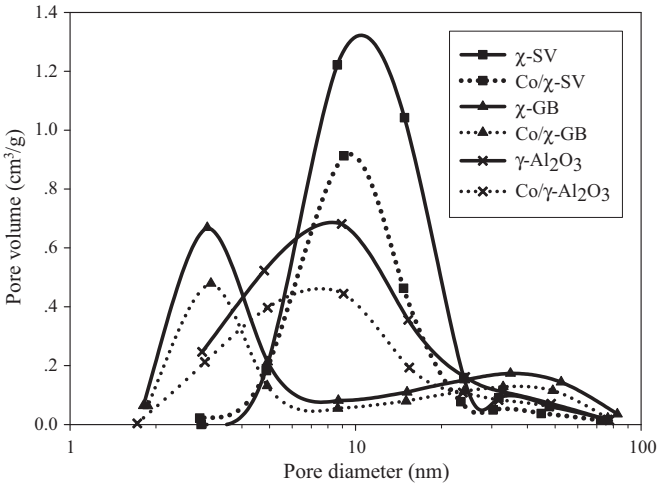

Fig. 2. The pore size distribution of Al_2O_3 and Co/Al_2O_3 catalysts.

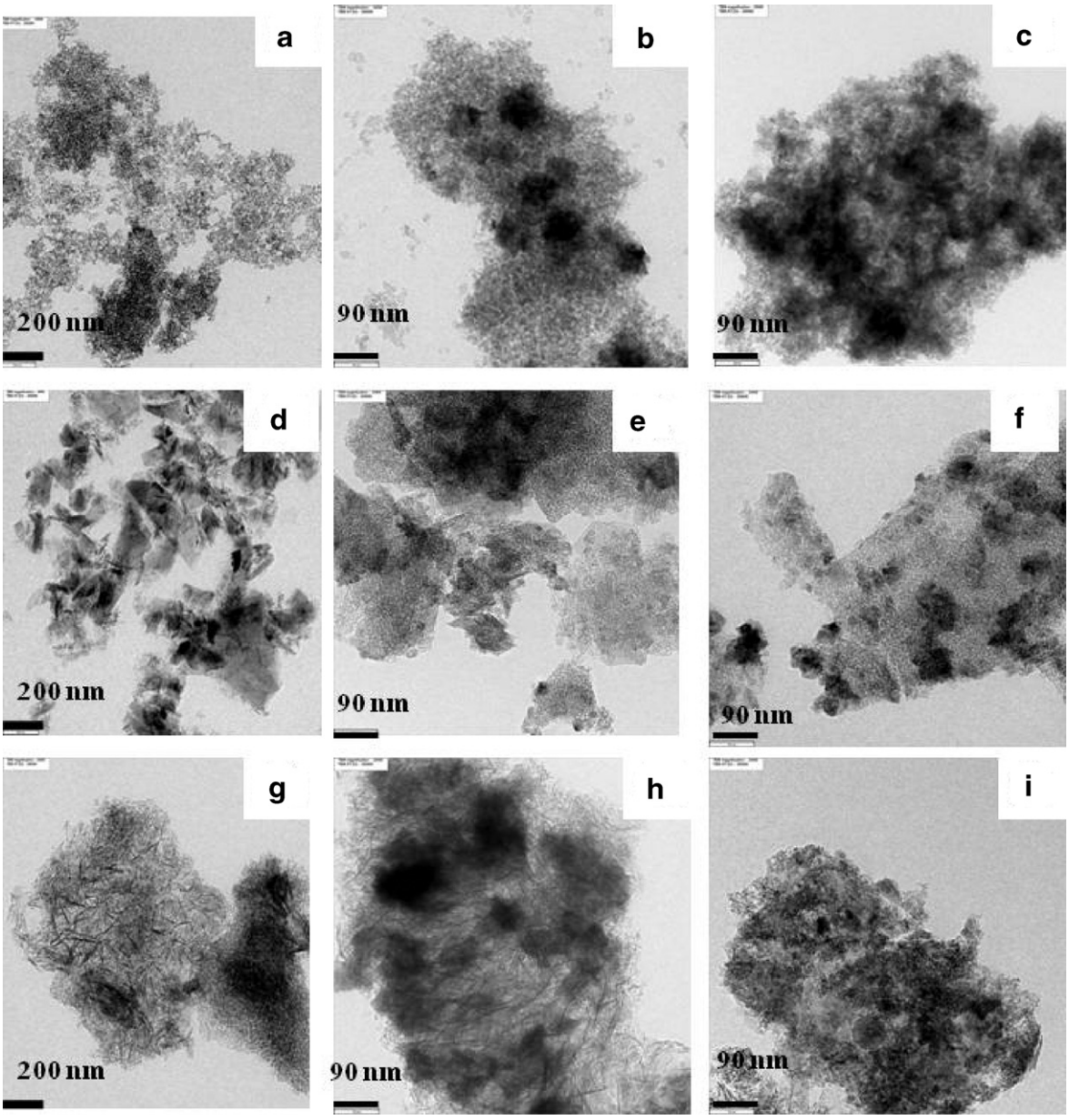

Fig. 3. The TEM micrographs of χ-SV (a), Co/χ-SV (b), used Co/χ-SV (c), χ-GB (d), Co/χ-GB (e), used Co/χ-GB (f), γ-Al_2O_3 (g), Co/γ-Al_2O_3 (h), and used Co/γ-Al_2O_3 (i).

γ-Al_2O_3 was unstable under hydrothermal conditions (>140 °C), resulting in an overgrowth of the surface crystallites [23].

The TPR profiles of the various Co/Al_2O_3 catalysts are shown in Fig. 4. The reduction peaks for bulk Co_3O_4 can be assigned to the two-step reduction of Co_3O_4 to CoO and then to Co^0 [24,25]. In the present work, the reduction peaks appeared at two major temperature ranges: 200–400 °C and 550–750 °C. According to the literature, the reduction of large Co_3O_4 particles to Co metal and possibly partial reduction of highly dispersed Co_3O_4 to CoO occurred at the lower temperature range whereas the higher reduction temperature at ca. 550–750 °C was assigned to the reduction of CoO (possibly) and Co species that are highly dispersed and strongly interacting with the Al_2O_3 support or the reduction of cobalt aluminate [26,27]. The reduction temperature for Co/χ-SV and Co/χ-GB was higher than that of Co/γ-Al_2O_3, indicating a stronger interaction between Co particles and χ-phase alumina. It has often been reported that the reduction temperatures of Co/Al_2O_3 decreased with increasing pore size of Al_2O_3 [18,26]. However, the reduction temperature of Co/χ-SV with relatively large pore size was shifted towards higher temperature, suggesting that the reduction behavior of cobalt on Al_2O_3 was also affected by the structure and morphology of the Al_2O_3 support.

The CO conversion, reaction rate, product selectivity, and turnover frequencies calculated from the CO chemisorption are given in Table 2. The time on stream results are also illustrated

Table 2
Catalytic activity of the Co/Al_2O_3 catalysts in CO hydrogenation.

Catalysts	CO conversion[a] (%)		Selectivity[b] (%)		TOF[c] ($\times 10^3$ s^{-1})
	Initial[d]	Steady-state[b]	C_1	C_2–C_4	
Co/χ-SV	84.1	78.8	99.5	0.5	10.2
Co/χ-GB	87.2	60.9	99.3	0.7	6.6
Co/γ-Al_2O_3	67.2	46.6	98.3	1.7	5.7

[a] The reaction conditions were 220 °C, 1 atm, and H_2/CO/Ar = 20/2/8.
[b] After 6 h time-on-stream.
[c] Based on CO chemisorption results.
[d] After 5 min time-on-stream.

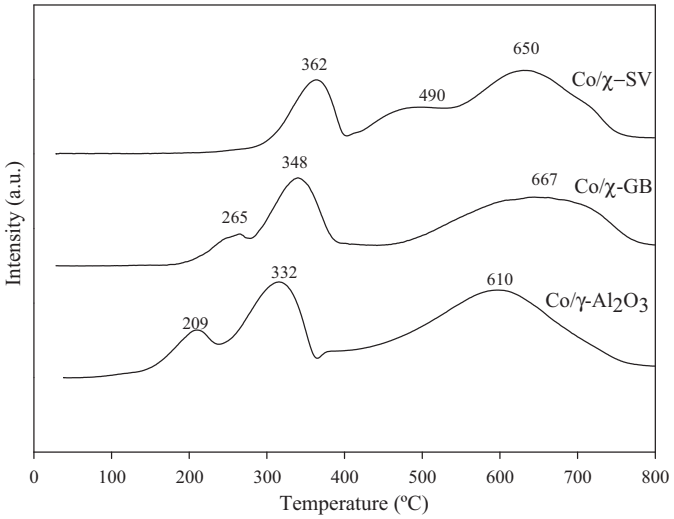

Fig. 4. The TPR profiles of the Co catalysts supported on χ-SV (a), χ-GB (b), and γ-Al_2O_3 (c).

in Fig. 5. The initial CO conversion was found to be in the order Co/χ-GB > Co/χ-SV > Co/γ-Al_2O_3, which was correlated well with the amount of cobalt active sites measured from CO chemisorption. However, as shown in the time-on-stream profiles and the steady-state values, the Co/χ-SV exhibited the highest CO conversion and methane selectivity after 6-h time-on-stream. The activity of Co/χ-SV decreased only by 6% whereas those of Co/χ-GB and Co/γ-Al_2O_3 decreased by ∼30%. It is suggested that the strong interaction between cobalt particles and the spherical shape χ-Al_2O_3 particles and/or the higher amount of aluminates formation provided better stabilization of cobalt particles during CO hydrogenation, preventing sintering of the catalysts as well as rearranging of active cobalt surface which was typically found in other supported cobalt catalyst systems [28–31]. There were no significant differences in turnover frequencies of the various Co/Al_2O_3 catalysts, confirming the structure insensitivity of the reaction [32–34].

The formation of inactive carbon species can be a reason for the catalyst deactivation. The TG/DTA experiments were carried out for all the spent catalysts in order to determine the amounts of carbonaceous deposits after CO hydrogenation reaction and the results are shown in Fig. 6. A small weight loss in the TGA profiles (Fig. 6a) below 200 °C was due to the removal of physisorbed water and/or chemisorbed hydroxyl groups whereas the weight loss at higher temperature was due to oxidation of the carbonaceous deposited on the surface of used catalysts [35]. As shown by the exothermic peaks in Fig. 6b, the type of coke species occurred during reaction was probably "soft coke" since it could be removed from the spent catalysts by oxidation at a relative lower temperature (∼350 °C) [36,37]. Based on the TG/DTA results, the amount of coke deposits on the catalysts prepared on χ-phase Al_2O_3 were much lower than that prepared on the γ-Al_2O_3 in the order: Co/χ-SV < Co/χ-GB < Co/γ-Al_2O_3. The results were in good agreement with the activity trend shown in Fig. 5 in which the activity of Co/χ-SV was the most stable during the 6 h time-on-stream. However, it should be noted that even though the catalytic properties of Co/χ-GB were not exactly the same as that of Co/χ-SV, the synthesis of high purity nanocrystalline χ-Al_2O_3 from the calcination of milled gibbsite (χ-GB) appeared to be much easier and more feasible than the solvothermal method and could be employed in a large scale production.

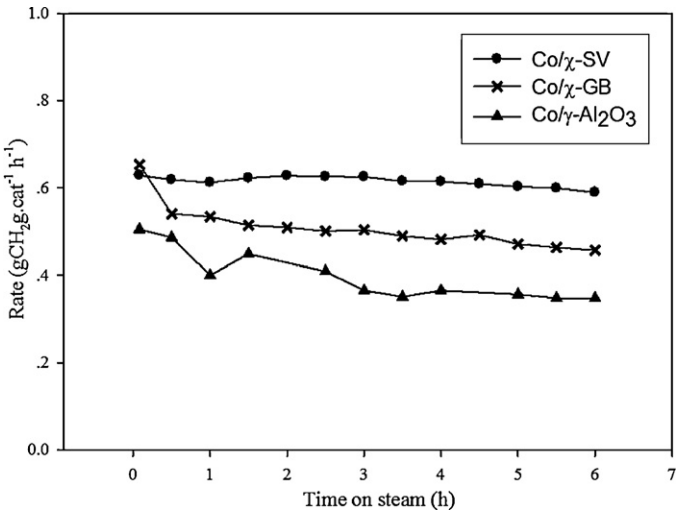

Fig. 5. The CO hydrogenation rate versus time-on-stream for the various Co/Al_2O_3 catalysts.

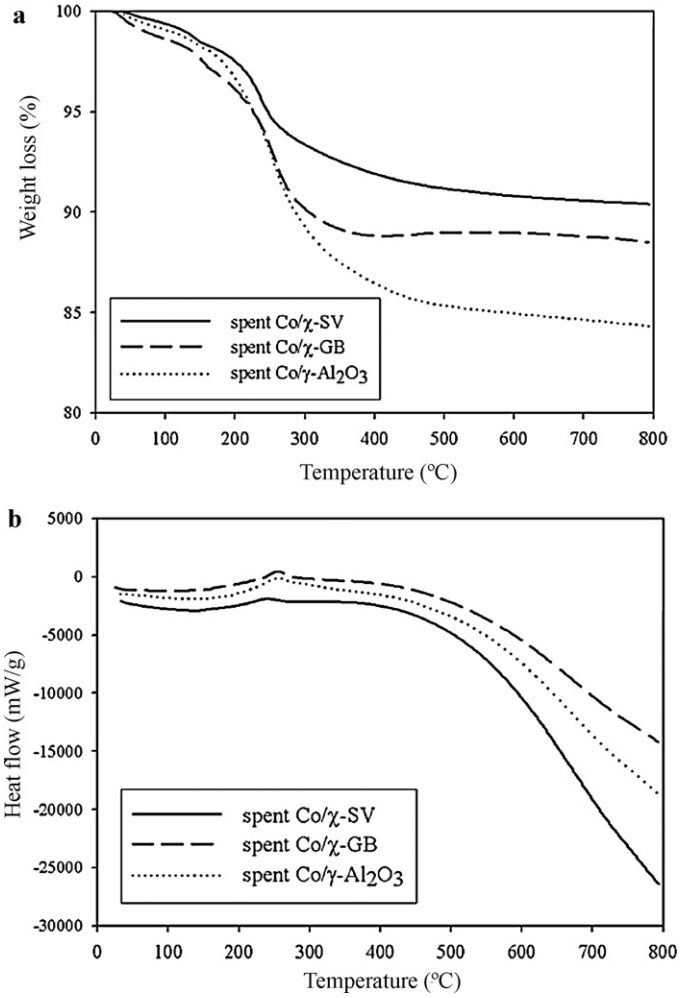

Fig. 6. The TG/DTA results of spent Co/Al_2O_3 catalysts after reaction: (a) in terms of temperature (°C) and weight loss (%); (b) in terms of temperature (°C) and heat flow (mW/g).

4. Conclusions

The Co catalysts supported on pure χ-phase and γ-phase Al_2O_3 were investigated in the CO hydrogenation. The nanocrystalline χ-Al_2O_3 was synthesized by two different routes namely

solvothermal method and thermal decomposition of fine gibbsite. Despite their similar BET surface area, the Co dispersion measured from CO chemisorption and initial CO hydrogenation rate increased in the order Co/χ-GB > Co/χ-SV > Co/γ-Al_2O_3. However, the Co/χ-SV exhibited the highest activity under steady-state conditions (only 6% decrease from the initial values) due probably to high thermal stability of the χ-SV alumina and stable cobalt particles on the catalyst surface. A stronger interaction between cobalt and χ-alumina was clearly observed by H_2-TPR. Moreover, the textural properties of χ-phase alumina were more stable than the γ-Al_2O_3 during CO hydrogenation.

Acknowledgments

Financial support from the Thailand Research Fund (TRF) grant number DBG52-Bunjerd Jongsomjit is gratefully acknowledged. The authors also would like to thank the Research Unit of Advanced Ceramic and Polymeric Materials, National Center of Excellence for Petroleum, Petrochemicals and Advanced Materials, Chulalongkorn University, Bangkok, Thailand for providing the attrition mill.

References

[1] C.J. Brinker, G.W. Scherrer, Sol-Gel Science, Academic Press, San Diego, 1990.
[2] K.-C. Song, K.-J. Woo, Y. Kang, Korean J. Chem. Eng. 16 (1) (1999) 75–81.
[3] S.G. Deng, Y.S. Lin, Sci. Lett. 16 (1997) 1291–1294.
[4] Y. Sarikaya, I. Sevinc, M. Akinc, Powder Technol. 116 (1) (2001) 109–114.
[5] S.-M. Oh, D.-W. Park, Korean J. Chem. Eng. 17 (3) (2000) 299–303.
[6] M. Inoue, H. Kominami, T. Inui, J. Am. Ceram. Soc. 75 (1996) 2597–2598.
[7] N. Wongwaranon, O. Mekasuwandumrong, P. Praserthdam, J. Panpranot, Catal. Today 131 (2008) 553–558.
[8] O. Mekasuwandumrong, N. Wongwaranon, P. Praserthdam, J. Panpranot, Mater. Chem. Phys. 111 (2008) 431–437.
[9] S. Komhom, O. Mekasuwandumrong, J. Panpranot, P. Praserthdam, Ind. Eng. Chem. Res. 48 (2009) 6273–6279.
[10] Y. Deng, G.-D. Wei, C.-W. Nan, Chem. Phys. Lett. 368 (2003) 639–643.
[11] Y. Deng, X.-S. Zhou, G.-D. Wei, J. Liu, C.-W. Nan, S.-J. Zhao, J. Phys. Chem. Solids 63 (2002) 2119–2121.
[12] K. Pansanga, J. Panpranot, O. Mekasuwandumrong, C. Satayaprasert, P. Praserthdam, Korean J. Chem. Eng. 24 (2007) 397–402.
[13] K. Pansanga, J. Panpranot, O. Mekasuwandumrong, C. Satayaprasert, G.J. Goodwin, P. Praserthdam, Catal. Commun. 9 (2008) 207–212.
[14] J. Khom-in, P. Praserthdam, J. Panpranot, O. Mekasuwandumrong, Catal. Commun. 9 (2008) 1955–1958.
[15] C. Meephoka, C. Chaisuk, P. Samparnpiboon, P. Praserthdam, Catal. Commun. 9 (2008) 546–550.
[16] W. Chaitree, S. Jiemsirilers, O. Mekasuwandumrong, T. Charinpanichkul, P. Praserthdam, J. Panpranot, J. Am. Ceram. Soc. 93 (2010) 3377–3383.
[17] O. Mekasuwandumrong, P.L. Silveston, P. Praserthdam, M. Inoue, V. Pavarajarn, W. Tanakulrungsank, Inorg. Chem. Commun. 6 (2003) 930.
[18] D. Xu, W. Li, H. Duan, Q. Ge, H. Xu, Catal. Lett. 102 (2005) 229–235.
[19] Ø. Borg, N. Hammer, S. Eri, O.A. Lindvåg, R. Myrstad, E.A. Blekken, M. Rønning, E. Rytter, A. Holmen, Catal. Today 142 (2009) 70–77.
[20] Ø. Borg, J.C. Walmsley, D. Royal, B.S. Tanem, E.A. Blekkan, S. Eri, E. Rytter, A. Holmen, Catal. Lett. 126 (2008) 224–230.
[21] P. Souza Santos, H. Souza Santos, S.P. Toledo, Mater. Res. 3 (2000) 104–114.
[22] S.-M. Kim, Y.-J. Lee, K.-W. Jun, J.-Y. Park, H.S. Potdar, Mater. Chem. Phys. 104 (2007) 56–61.
[23] L. Jun-Cheng, X. Lan, X. Feng, W. Zhan-Wen, W. Fei, Appl. Surf. Sci. 253 (2006) 766–770.
[24] D. Schanke, S. Vada, E.A. Blekkan, A. Hilmen, A. Hoff, A. Holmen, J. Catal. 156 (1995) 85.
[25] Y. Zhang, D. Wei, S. Hammache, J.G. Goodwin Jr., J. Catal. 188 (1999) 281.
[26] H. Xiong, Y. Zhang, S. Wang, J. Li, Catal. Commun. 6 (2005) 512–516.
[27] S. Rojanapipatkul, B. Jongsomjit, Catal. Commun. 10 (2008) 232–236.
[28] W.J. Bae, M.S. Kim, J.Y. Lee, J.M. Lee, W.K. Jun, Catal. Commun. 10 (2009) 1358–1362.
[29] Z. Yan, Z. Wang, D.B. Bukur, D.W. Goodman, J. Catal. 268 (2009) 196–200.
[30] D.J. Duvenhageand, N.J. Coville, Appl. Catal. A 289 (2005) 231–239.
[31] B. Jongsomjit, T. Wongsalee, P. Praserthdam, Mater. Chem. Phys. 97 (2006) 343–350.
[32] A. Kogelbauer, J.G. Goodwin Jr., R. Oukaci, J. Catal. 160 (1996) 125–133.
[33] B. Jongsomjit, J.G. Goodwin Jr., Catal. Today 77 (2002) 191–204.
[34] S. Kittiruangrayab, T. Burakorn, B. Jongsomjit, P. Praserthdam, Catal. Lett. 124 (2008) 376–383.
[35] R.W. Soares, V.J. Menezes, M.V.A. Fonseca, J. Dweck, J. Therm. Anal. 49 (1997) 657–661.
[36] M.R. Jovanović, P.S. Putanov, Appl. Catal. A 159 (1997) 1–7.
[37] X. Zhang, Y. Wang, F. Xin, Appl. Catal. A 307 (2006) 222–230.